Volume 305, number 2, 137–143 FEBS 11203 June 1992

Stereospecific assignments and $\chi 1$ rotamers for FKBP when bound to ascomycin from $^3J_{H^\alpha,H^\beta}$ and $^3J_{N,H^\beta}$ coupling constants

Robert X. Xu, Edward T. Olejniczak and Stephen W. Fesik

Pharmaceutical Discovery Division, Abbott Laboratories, Abbott Park, IL 60064, USA

Received 1 May 1992

$^3J_{H^\alpha,H^\beta}$ and $^3J_{N,H^\beta}$ coupling constants were measured for isotopically labeled FKBP when bound to the immunosuppressant, ascomycin, using a ^{1}H-coupled 3D HCCH-TOCSY and ^{15}N-coupled 3D HSQC-TOCSY experiment, respectively. From an analysis of these two sets of coupling constants, stereospecific β-proton assignments and $\chi 1$ rotamers for FKBP have been obtained. All of the $\chi 1$ rotamers were consistent with the $\chi 1$ angles measured in the X-ray crystal structure of the FKBP/FK506 complex, suggesting that the structures of the two complexes are similar.

FKBP; Ascomycin; Coupling constant; NMR

1. INTRODUCTION

The accuracy and precision of 3D structures determined by NMR have dramatically improved in the last few years [1]. These improvements are largely due to an increase in the number of proton–proton distance constraints obtained from NOE data. Although homonuclear and heteronuclear three-bond coupling constants could also be used to obtain additional dihedral angle constraints to further improve the quality of structures determined by NMR, it is difficult to obtain these J-couplings in large systems due to the broad linewidths of the NMR signals and spectral overlap. Recently, elegant experimental approaches have been devised to overcome some of the limitations for measuring J-couplings in large molecules [2–7]. However, only a few selected examples of coupling constants have been measured using these techniques, and in many cases, no useful applications of the methods have been reported.

In this paper, we describe a 3D NMR method for measuring three-bond proton–proton coupling constants in ^{13}C-labeled proteins that is based on previously reported 2D NMR experiments [5,6]. Using this technique, we have measured the $^3J_{H^\alpha,H^\beta}$ coupling constants for [U-^{15}N,^{13}C]FKBP (FK506 binding protein; 11.8 kDa) [8,9] when bound to the immunosuppressant, ascomycin [10,11]. In addition, we have measured the $^3J_{N,H^\beta}$ coupling constants in the [U-^{15}N]FKBP/ascomycin complex using a ^{15}N-coupled 3D HSQC-TOCSY experiment [2]. From an analysis of these two sets of coupling constants, the stereospecific assignments for most of the β-protons of FKBP have been determined which is important for accurately interpreting the NOEs involving these protons. In addition, $\chi 1$ rotamers consistent with the coupling constants were obtained, providing additional restraints for the structure determination of the FKBP/ascomycin complex. The $\chi 1$ rotamers determined by NMR for the FKBP/ascomycin complex in solution were compared to the $\chi 1$ angles determined in the X-ray crystal structure of the FKBP/FK506 complex [12].

Abbreviations: NOE, nuclear Overhauser effect; FKBP, FK506 binding protein; 3D HSQC-TOCSY, three-dimensional heteronuclear single quantum correlation-total correlation spectroscopy; 3D HCCH-TOCSY, three-dimensional ^{1}H-^{13}C-^{13}C-^{1}H correlation via ^{13}C total correlation spectroscopy; E.COSY, exclusive correlation spectroscopy.

Correspondence address: S.W. Fesik, Pharmaceutical Discovery Division, D-47G, AP9, Abbott Laboratories, Abbott Park, IL 60064, USA. Fax: (1) (708) 938-2478.

2. MATERIALS AND METHODS

2.1. *Materials*

Recombinant human FKBP was cloned from a Jurat T cell cDNA library and expressed in *E. coli* using the PKK233-3 vector containing a *trc* promoter [13]. [U-^{15}N]FKBP was prepared by growing cells on a minimal medium containing ^{15}N ammonium chloride as the nitrogen source, and [U-^{15}N,^{13}C]FKBP was prepared from cells grown on ^{15}N ammonium chloride and [U-^{13}C]acetate. FKBP was purified from these cells as previously described [13].

2.2. *NMR sample preparation*

The NMR samples (3 mM) of the uniformly ^{15}N and ^{15}N,^{13}C FKBP/ascomycin complex were prepared in an H_2O or D_2O buffer (pH 6.5), respectively, containing 50 mM potassium phosphate, 100 mM sodium chloride, and 5 mM dithiothreitol-d_{10}. To form the complex, excess unlabeled ascomycin was incubated with the protein solution for 24–48 h at room temperature.

2.2. *NMR experiments*

The NMR data were acquired on a Bruker AMX500 (500 MHz) NMR spectrometer at 30°C and processed using in-house written software on Silicon Graphics computers. Linear Prediction was employed to improve windowing and resolution in the indirect detected dimensions [14]. The time domain data in the indirect detected dimensions was extended by one quarter of the number of experimental points. Data sets were extensively zero filled to aid in the interpolation of the peak positions.

The $^3J_{H^\alpha,H^\beta}$ coupling constants were measured using a ^{1}H-coupled 3D HCCH-TOCSY experiment [15] in which a small flip angle pulse was used in the reverse INEPT part of the experiment as shown in Fig. 1A. The data set contained $47(t_1) \times 48(t_2) \times 1024(t_3)$ complex points which were acquired using spectral widths of 3704 Hz (ω_1, ^{1}H), 4167 Hz (ω_2, ^{13}C), and 8333 Hz (ω_3, ^{1}H). The ω_2 dimension was folded once. The final data set size after zero-filling was $128(\omega_1) \times 256(\omega_2) \times 8192(\omega_3)$ points, giving a final digital resolution in ω_3 of 1.0 Hz per point. A DIPSI-2 [16] spinlock mixing period of 7.8 ms, and a τ_1, τ_2 value of 1.5 ms was employed. Thirty-two transients were accumulated per increment with a 1.1 s relaxation delay between scans. The total accumulation time was 3.5 days.

The $^3J_{N,H^\beta}$ coupling constants were measured using a ^{15}N-coupled 3D HSQC-TOCSY experiment [2] with the pulse sequence shown in Fig. 1B. The data set contained $33(t_1) \times 48(t_2) \times 1024(t_3)$ complex points which were acquired using spectral widths of 1773 Hz (ω_1, ^{15}N), 3205 Hz (ω_2, $^1H^N$), and 10,000 Hz (ω_3, ^{1}H). The final data set size after zero-filling was $128(\omega_1) \times 256(\omega_2) \times 16834(\omega_3)$ points, giving a final digital resolution in ω_3 of 0.6 Hz per point. An MLEV-17 mixing scheme of 48 ms was employed which was modified for the suppression of rotating frame NOE contributions [17], and water suppression was accomplished with a 2 ms spinlock using the method of Messerle et al. [18]. The water streak was further reduced during data processing by using a time domain filter in which linear prediction was used to extrapolate the filter for the initial time domain points. Thirty-two transients were accumulated per increment with a 1.1 s relaxation delay between scans. The total accumulation time was 2.5 days.

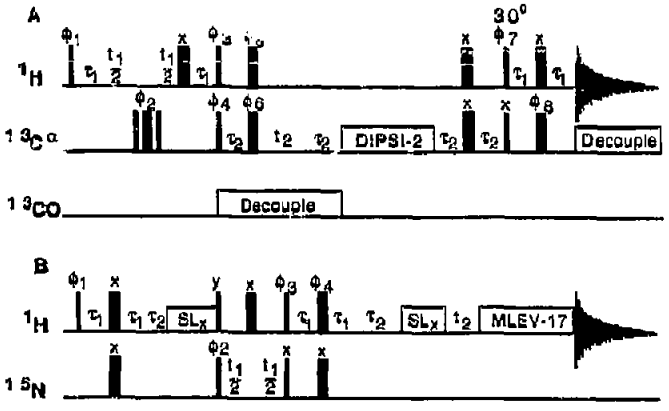

Fig. 1. (A) Pulse sequence for the ^{1}H-coupled 3D HCCH-TOCSY experiment. Wide bars correspond to 180° pulses and narrow bars denote 90° pulses except for the small flip angle (30°) in the reverse INEPT part of the experiment. The phase cycling for the pulses consists of $\phi1 = (x,x,-x,-x)$, $\phi2 = (x,-x)$, $\phi3 = (y,-y)$, $\phi4 = 8(x),8(-x)$, $\phi6 = (2x,2y,2(-x),2(-y))$, $\phi5 = (4x,4y,4(-x),4(-y))$, $\phi7 = (x,x,-x,-x)$, and $\phi8 = (4x,4y)$ with the receiver cycled $2(x,-x,-x,x),2(-x,x,x,-x)$. Quadrature in t_1 and t_2 was obtained using States TPPI [26] by incrementing $\phi1$ for t_1 and $\phi4$ for t_2. The carbon and proton carrier frequency was set at 52 and 3.13 ppm, respectively. (B) Pulse sequence for the 3D ^{15}N-coupled HSQC-TOCSY experiment with phase cycling: $\phi1 = (x,x,-x,-x)$, $\phi2 = (x,-x)$, $\phi3 = 4(x),4(-x)$, $\phi4 = 8(x),8(-x)$ with the receiver cycled $x,-x,-x,x,-x,x,x,-x$. Quadrature in t_1 and t_2 was obtained using States-TPPI [26] by incrementing $\phi2$ for t_1 and $\phi3$ for t_2. The proton carrier frequency was placed in the middle of the amides at 7.68 ppm. The τ_1 delay (2.7 ms) was set to $1/4(^1J_{NH})$, and τ_2 was added to compensate for the length of the 90° proton pulse.

3. RESULTS AND DISCUSSION

3.1. *Measurement of $^3J_{H^\alpha,H^\beta}$ coupling constants*

Fig. 1A depicts the 3D HCCH-TOCSY pulse sequence used in measuring the $^3J_{H^\alpha,H^\beta}$ coupling constants of [U-^{13}C,^{15}N]FKBP when bound to ascomycin. After frequency labeling the protons during the t_1 period, the magnetization is transferred by an INEPT experiment to the attached carbon which is indirectly detected during t_2. A DIPSI-2 mixing scheme [16] is used to transfer magnetization between carbons followed by a reverse INEPT sequence and the detection of the protons during the acquisition (t_3) period. No proton decoupling was employed during t_2 to preserve the large $^1J_{^{13}C,^1H}$ coupling important in these E.COSY-type experiments [2–7]. In order to avoid mixing the spin states, either a selective proton 90° pulse [5] or a small flip angle pulse [6,7] could be used in the reverse INEPT part of the experiment. We chose to use a small flip angle pulse to eliminate the problems associated with selectively perturbing protons in crowded spectral regions, with the added advantage of allowing all of the J-couplings to be measured in a single experiment.

Representative $^{13}C(\omega_2)$,$^1H(\omega_3)$ planes extracted from the 3D NMR experiment at different proton chemical shifts (ω_1) are shown in Fig. 2. The $^3J_{H^\alpha,H^\beta}$ coupling constants are obtained from these spectra by measuring the frequency difference in ω_3 between the two ^{13}C-coupled α-proton peaks (ω_2). In order to obtain an accurate and reproducible measure of these couplings, several methods were tried. The most reliable approach was to extract and simultaneously display on a graphics screen the 1D ω_3 traces of the 3D data at the center of each of the peaks split by the large one-bond ^{13}C-^{1}H coupling. The coupling constants were measured by shifting one of the traces relative to the other until the peaks overlap, with the amount of the shift corresponding to the coupling constant.

Using this approach, both $^3J_{H^\alpha,H^\beta}$ coupling constants could be measured (Table I) for thirty-six of the sixty-one amino acid residues that contain two β-protons (excluding proline). $^3J_{H^\alpha,H^\beta}$ coupling constants could not be measured for ten of these amino acids due to degenerate β-methylene protons and for another nine due to spectral overlap. For amino acid residues Val, Ile, and Thr that contain only one β-proton, coupling constants were measured for twenty out of twenty-one of these spin systems. Of these, only the $^3J_{H^\alpha,H^\beta}$ coupling constant of T14 could not be measured as a result of spectral overlap with the water resonance.

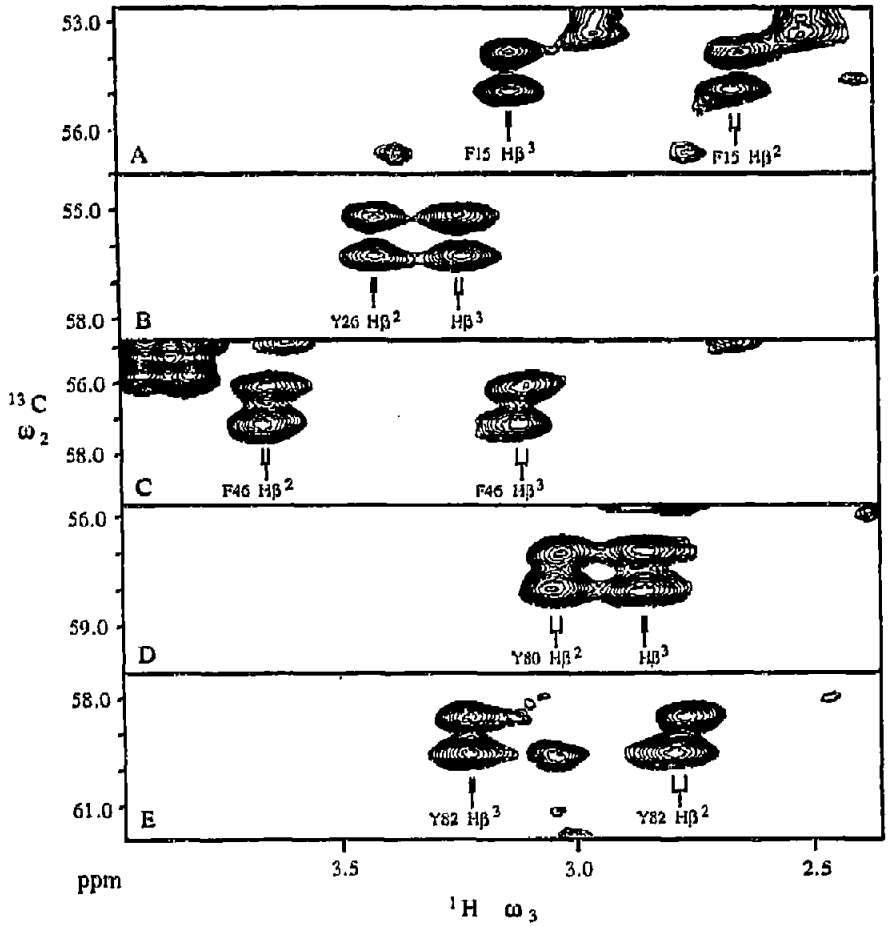

Fig. 2. $^{13}C(\omega_2)$,$^1H(\omega_3)$ planes from the ^1H-coupled 3D HCCH-TOCSY spectrum extracted at (A) 5.27, (B) 6.72, (C) 4.98, (D) 4.49, (E) 4.28 ppm (ω_1). $^3J_{H^\alpha,H^\beta}$ coupling constants are measured from the frequency difference in ω_3 between the two ^{13}C-coupled α-proton peaks (ω_2).

3.2. *Measurement of* $^3J_{N,H^\beta}$ *coupling constants*

The $^3J_{N,H^\beta}$ coupling constants for the [U-^{15}N]FKBP/ascomycin complex were measured using the 3D ^{15}N-resolved HSQC-TOCSY pulse sequence [2] shown in Fig. 1B. No ^{15}N decoupling was employed during the t_2 period, generating two peaks separated by the large $^1J_{N,H^N}$ coupling constant from which the $^3J_{N,H^\beta}$ couplings were measured [2]. Fig. 3 depicts a $^1H(\omega_2)$,$^1H(\omega_3)$ plane from the 3D HSQC-TOCSY experiment extracted at the $^{15}N(\omega_1)$ chemical shift of 123.0 ppm. The $^3J_{N,H^\beta}$ coupling constants were measured from the 3D NMR spectrum from the frequency difference in ω_3 between the peaks split by the large one-bond ^{15}N,^{1}H coupling in ω_2 by the method of shifting the 1D traces as previously described for the $^3J_{H^\alpha,H^\beta}$ measurements. As shown in Table I, most of the possible $^3J_{N,H^\beta}$ coupling constants could be measured using this technique.

3.3. *Stereospecific assignments and* $\chi 1$ *angles*

In previous NMR studies, the stereospecific β-proton assignments and $\chi 1$ angles were determined from an analysis of *both* coupling constants and NOE data [19–21]. In principle, if all four $^3J_{H^\alpha,H^\beta}$ and $^3J_{N,H^\beta}$ coupling constants can be measured, the $\chi 1$ angle and stereospecific assignments of the β-protons could be made independent of the NOE data. As shown in Fig. 4, two small $^3J_{H^\alpha,H^\beta}$ coupling constants (<5.5 Hz) are indicative of a g$^-$ rotamer [22] ($\chi 1 = +60°$) with the stereospecific β-proton assignments defined by the $^3J_{N,H^\beta}$ coupling constants (>4.0 Hz, $H^{\beta 2}$; <2.5 Hz, $H^{\beta 3}$). Two small $^3J_{N,H^\beta}$ coupling constants (< 2.5 Hz) support a t rotameric state ($\chi 1 = 180°$) with the stereospecific β-proton assignments defined by the $^3J_{H^\alpha,H^\beta}$ coupling constants (<5.5 Hz, $H^{\beta 2}$; >9.0 Hz, $H^{\beta 3}$). The g$^+$ rotamer is supported by one big and one small $^3J_{H^\alpha,H^\beta}$ and $^3J_{N,H^\beta}$ coupling constant.

From a qualitative analysis of the coupling constants given in Table I, the stereospecific β-proton assignments and preferred $\chi 1$ rotamers were determined for the individual amino acids of FKBP when bound to ascomycin. As shown in Table I, a single rotamer was determined for most of the amino acids using only the coupling constant data. In those cases in which one or more of the coupling constants could not be measured as for

T14, C22, R40, D41, E54, V55, I56, Q65, and M66, two $\chi 1$ rotamers were found to be consistent with the J-couplings, eliminating only one of the possible rotamers. In other cases such as for S8, R13, K34, K52, and E107, the coupling constants did not support *any* of the possible $\chi 1$ rotamers. Additional stereospecific assignments and $\chi 1$ rotamers are also listed in Table I that could not be determined solely from the coupling constants but required the NOE data (asterisks).

For a more quantitative analysis of the coupling constant data, the $^3J_{H^\alpha,H^\beta}$ and $^3J_{N,H^\beta}$ coupling constants were compared to those predicted by the Karplus equations [20,23]:

$$^3J_{H^\alpha,H^\beta} = 9.5\cos^2(\chi 1+240°)-1.6\cos(\chi 1+240°)+1.8$$

$$^3J_{H^\alpha,H^\beta} = 9.5\cos^2(\chi 1)-1.6\cos(\chi 1)+1.8$$

$$^3J_{N,H^\beta} = -4.4\cos^2(\chi 1+120°)+1.2\cos(\chi 1+120°)+0.1$$

$$^3J_{N,H^{\beta'}} = -4.4\cos^2(\chi 1-120°)+1.2\cos(\chi 1-120°)+0.1$$

In order to partially compensate for errors in the parameterization of the Karplus equations, the possibility of restricted motional averaging, and the digital resolution of the spectra, $\chi 1$ values were accepted in which $|J_{observed}-J_{predicted}|$ was less than +/−2 Hz for $^3J_{H^\alpha,H^\beta}$ and +/−1 Hz for $^3J_{N,H^\beta}$. Predicted $\chi 1$ values within 20° of an eclipsed conformation were eliminated due to their high energy and to the fact that they are rarely observed in protein structures previously determined by X-ray crystallography [21,24].

As shown in Table I, for several of the residues no $\chi 1$ angle could be found that satisfied these criteria. Moreover, many of the $\chi 1$ angles that could be fit to the

Table I

$^3J_{H^\alpha,H^\beta}$ and $^3J_{N,H^\beta}$ coupling constants from which stereospecific β-proton assignments and $\chi 1$ rotamers/angles were determined. For comparison, the $\chi 1$ angles measured in the X-ray structure of the FKBP/FK506 complex [12] are listed

	δ (ppm)		^3J (Hz)				$\chi 1$		
res	$H^{\beta 2}$	$H^{\beta 3}$	$H^\alpha,H^{\beta 2}$	$H^\alpha,H^{\beta 3}$	$N,H^{\beta 2}$	$N,H^{\beta 3}$	Rotamer	NMR	X-ray
V2	–	1.89	–	3.1	–	0.7	g^-	64 ± 16	58
Q3	1.99	2.13	9.2	o	1.2	4.9	g^+		–59
V4	–	2.05	–	10.2	–	m	t		176
E5	d	d							–67
T6	4.10	–	10.7	–	m	–	g^+		–68
I7	1.35	–	13.2	–	2.2	–	g^+	–78 ± 2	–65
S8			4.0[a]	2.0	1.8[a]	1.8			–42
D11	3.02	2.77	5.5	2.0	5.6	2.3	g^-	80 ± 4	70
R13	1.78*	1.58*	5.1	3.0	2.4	1.2	g^-*		–175
T14	4.28	–	o	–	1.2	–	g^+*/t		–43
F15	2.64	3.12	9.0	2.0	1.2	4.8	g^+	–88± 2	–66
K17	1.57	1.86	11.0	3.2	1.2	4.0	g^+	–84 ± 4	–71
R18	d	d							–155
Q20	2.29	1.94	m	4.1	0.6	5.8	g^+		–66
T21	3.95	–	10.6	–	2.2	–	g^+	–85 ± 16	–65
C22	2.18*	2.00*	o	o	1.1	5.2	g^+*/g^-		–56
V23	–	2.08	–	10.2	–	1.2	t	–162 ± 10	–176
V24	–	2.55	–	4.3	–	4.3	g^+	–44 ± 4	–52
H25			o	o	1.2[a]	1.8	t		–100
Y26	3.40	3.24	2.0	4.0	5.6	1.2	g^-	60 ± 4	70
T27	4.11	–	9.0	–	1.2	–	g^+	–86 ± 4	–62
M29	1.99*	1.87*	2.0	2.0	m	m	g^-		65
L30	2.23	1.97	11.6	4.2	1.8	4.3	g^+	–72 ± 0	–74
E31	d	d							–93
D32	3.01	2.64	3.0	4.0	4.3	1.8	g^-	72 ± 2	62
K34			3.0[a]	8.1	0.6[a]	2.4			–108
K35	d	d							–173
F36	3.36	2.73	4.0	4.0	4.8	0.6	g^-	60 ± 12	53
D37	3.61	2.63	5.0	10.0	1.2	0.6	t	–176 ± 8	–173
S38	4.12	3.65	3.0	9.1	1.8	0.6	t	–146 ± 8	173
S39	5.03*	3.24*	3.0	2.0	m	m	g^-		59
R40	1.45*	1.49*	14.0	2.0	o	o	g^+*/t		–66
D41	2.82*	2.73*	o	o	5.4	0.6	g^-*/g^+		–67
R42	d	d							–62
N43	3.24*	2.71*	5.0	3.1	1.0	0.8	g^-*		–71
K44	1.70*	1.84*	o	o	0.3	1.8	t		177
F46	3.65	3.11	5.0	9.1	1.8	0.6	t		170
K47	1.52*	1.29*	10.1	5.0	0.6	2.4	g^+*		–60

Table I (cont.)

	δ (ppm)		^3J (Hz)				$\chi 1$		
res	$H^{\beta 2}$	$H^{\beta 3}$	$H^{\alpha},H^{\beta 2}$	$H^{\alpha},H^{\beta 3}$	$N,H^{\beta 2}$	$N,H^{\beta 3}$	Rotamer	NMR	X-ray
F48	2.95	2.89	3.0	3.0	5.4	1.8	g^-	70 ± 2	70
M49	1.98	2.13	11.0	3.0	1.2	4.2	g^+	−82 ± 8	−69
L50	1.93	1.26	10.0	3.0	2.4	5.5	g^+	−82 ± 6	−97
K52	1.76*	2.13*	5.0	3.0	1.7	4.1	g^{+}*		−78
Q53	d	d							−69
E54			o	o	0.6[a]	4.2	g^+/g^-		−79
V55	–	1.42	–	5.0	–	m	g^{+}*/g^-		−74
I56	2.33	–	2.0	–	m	–	g^{-}*/t		49
R57	1.82*	1.38*	m	m	m	m	t*		−177
W59	3.01	2.66	9.1	m	2.4	4.8	g^+		−93
E60	d	d							−177
E61	1.91	2.21	13.0	4.1	1.8	4.2	g^+	−72 ± 2	−70
V63	–	2.27	–	13.6	–	2.0	t	166 ± 4	176
Q65	2.15*	2.43*	m	m	0.6	2.4	g^{+}*/t		−63
M66	2.15*	1.99*	m	m	1.7	5.7	g^{+}*/g^-		−64
S67	2.41	3.76	5.1	3.0	4.2	1.2	g^-	80 ± 4	58
V68	–	1.86	–	10.5	–	m	t		180
Q70	d	d							−172
R71	1.62	1.88	o	4.1	2.4	2.4	t		−174
K73	1.67	1.79	11.1	3.0	1.2	3.6		−88 ± 0	−89
L74	1.76	1.27	12.2	3.0	1.2	3.6	g^{+}*	−88 ± 0	−51
T75	4.04	–	9.1	–	2.2	–	g^+	−94 ± 12	−61
I76	1.92	–	13.2	–	0.0	–	g^+	−60 ± 20	−64
S77	4.44*	3.98*	4.0	1.0	m	m	g^-		62
D79	2.79	2.88	5.0	1.0	5.4	1.2	g^-	74 ± 12	45
Y80	3.05	2.86	12.0	3.0	2.4	4.4	g^+	−84 ± 4	−86
Y82	2.78	3.24	13.2	1.1	0.6	5.4	g^+	−72 ± 12	−55
T85	4.31	–	10.9	–	1.8	–	g^+	−80 ± 12	−56
H87	1.71*	2.35*	o	o	1.2	1.2	t		−177
I90	1.42	–	12.3	–	1.2	–	g^+	−72 ± 16	−51
I91	1.42	–	10.2	–	2.4	–	g^+	−88 ± 12	−68
H94	d	d							−50
T96	4.02	–	10.5	–	1.2	–	g^+	−76 ± 16	−68
L97	1.86	1.52	11.1	4.0	1.2	4.9	g^+	−62 ± 10	−55
V98	–	1.79	–	10.1	–	2.4	t	152 ± 12	180
F99	2.84	2.99	12.1	2.4	1.8	3.6		−88 ± 4	−76
D100	2.50	2.93	2.0	10.0	0.6	0.6	t	−160 ± 0	179
V101	–	1.67	–	10.2	–	1.2	t	156 ± 12	−179
E102	1.64*	2.10*	m	m	1.2	m	t		−172
L103			m	m	m				175
L104	d	d							−50
K105			o	o	o	o	g^{-}*		54
L106	1.58	1.23	12.2	3.0	0.6	4.8	g^+	−64 ± 12	−62
E107			3.0[a]	7.0	2.4[a]	1.2			−48

d, degenerate; *, derived from NOE data; a, lower field resonance; o, overlap with other peaks or noise; m, missing signal.

coupling constant data were outside of the range (60°, −60°, or 180° +/− 20°) typically observed in X-ray crystal structures [21,24]. Although the manner in which the coupling constants were analyzed is biased (i.e. it is easier to satisfy the criteria for angles larger than 60° or −60°), motional averaging and inaccuracies in the parameterization of the Karplus equations may also play a role. In addition to small angular fluctuations, large angular motions between different rotamers are possible. In an attempt to account for averaging between different rotamers, the NMR data were analyzed in terms of rotamer populations on the assumption that the observed coupling constants are due to an average of the values observed for the g^+, g^- and t rotamers as typically employed in the analysis of peptides [25]. However, for proteins, these assumptions may not be justified, since packing interactions may cause deviations from the standard rotamer geometries which would result in coupling constants outside of the range allowed by this model. Nevertheless, we analyzed both $^3J_{H^{\alpha},H^{\beta}}$ and $^3J_{N,H^{\beta}}$ (Table I) using this approach to determine if the data is qualitatively consistent with a preferred ro-

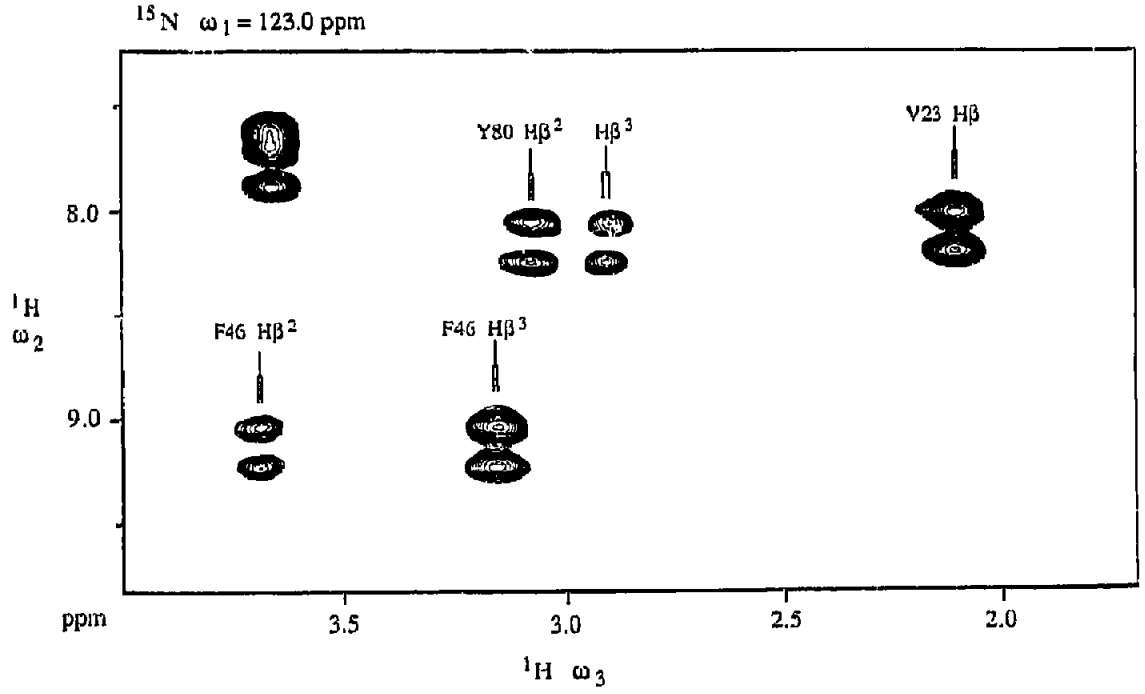

Fig. 3. $^1H(\omega_2)$,$^1H(\omega_3)$ cross-section from the ^1H-coupled 3D HSQC-TOCSY spectrum extracted at 123.0 ppm (ω_1) that depicts H^N,H^β cross-peaks. $^3J_{N,H^\beta}$ coupling constants are measured from the frequency difference in ω_3 between the two ^{15}N-coupled amide proton peaks (ω_2).

tamer. As expected, the rotamer with the greatest population was generally in agreement with the $\chi 1$ values predicted by the Karplus equations. However, exceptions were noted for those residues (S8, R13, N43, K34, K47, K52, and E107) that could not be fit to any $\chi 1$ angle. For these residues a preferred rotamer (>60%) could not be found that was consistent with both the $^3J_{H^\alpha,H^\beta}$ and $^3J_{N,H^\beta}$ data.

Since the amino acid residues on the surface of the protein may be expected to be more flexible than the buried residues, our NMR data were compared to the solvent accessibility of the FKBP residues determined in a preliminary NMR structure of the FKBP/ascomycin complex. As shown in Fig. 5, those residues in which four coupling constants were measured but could not be fit using the Karplus equations to a single $\chi 1$ angle (hatched bars) were all found on the surface of the protein. In addition, it is interesting to note that with the exception of Q70, the FKBP residues with degenerate β-protons were found to be solvent exposed (Fig. 5, solid bars).

3.4. *Comparison to the X-ray structure of FKBP/FK506*

The $\chi 1$ rotamers determined from the coupling constants and NOE data for FKBP when bound to ascomycin were compared to the $\chi 1$ angles measured in the X-ray structure of the FKBP/FK506 complex [12]. As shown in Table I, all of the $\chi 1$ rotamers that could be determined from the NMR data were in agreement with the $\chi 1$ angles in the X-ray structure. These results suggest that the solution and crystal structures are very similar. The only difference in which the NMR data were inconsistent with the X-ray structure was for some of the FKBP residues located on the surface of the protein. Although the $\chi 1$ angles were defined for these residues in the X-ray structure, the coupling constant data could not be fit to a single $\chi 1$ rotamer indicative of conformational averaging.

4. CONCLUSIONS

A ^{1}H-coupled 3D HCCH-TOCSY experiment is described for measuring $^3J_{H^\alpha,H^\beta}$ coupling constants in ^{13}C-labeled molecules. Using this technique $^3J_{H^\alpha,H^\beta}$ coupling

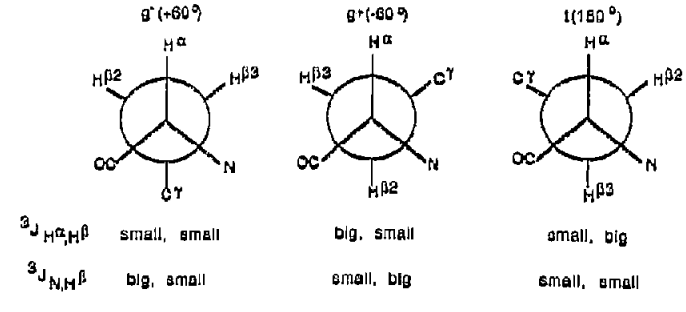

Fig. 4. Staggered rotamers g^-, g^+, and t corresponding to $\chi 1$ angles +60°, −60°, and 180°, respectively [22]. $^3J_{H^\alpha,H^\beta}$ (small < 5.5 Hz, big > 9.0 Hz) and $^3J_{N,H^\beta}$ (small < 2.5 Hz, big > 4.0 Hz) coupling constants that support the individual rotamers.

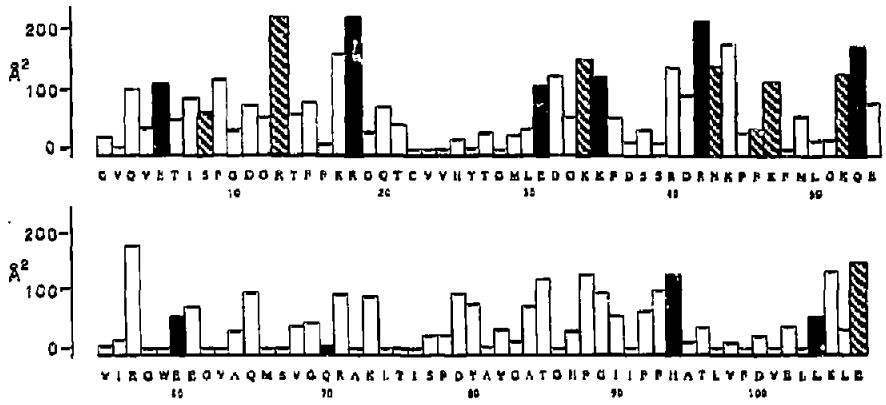

Fig. 5. Solvent accessibility (Å²) determined from a preliminary NMR structure of the FKBP/ascomycin complex. The solid bars correspond to amino acid residues with degenerate β-protons, and the hatched bars indicate FKBP residues in which four coupling constants were measured but were found to be inconsistent with a single $\chi 1$ angle.

constants were measured for [U-^{13}C,^{15}N]FKBP when bound to ascomycin. In addition, $^{3}J_{N,H^{\beta}}$ coupling constants were measured for the [U-^{15}N]FKBP/ascomycin complex using an ^{15}N-coupled 3D HSQC-TOCSY experiment [2]. From a qualitative analysis of this data, stereospecific β-proton assignments and $\chi 1$ rotamers were obtained which will be important for accurately defining a 3D structure of the FKBP/ascomycin complex in solution. All of the $\chi 1$ rotamers derived from the coupling constants and NOE data were in agreement with those obtained from the X-ray structure of the FKBP/FK506 complex [12], suggesting that the structures of the two complexes are very similar.

Acknowledgements: We thank Harriet Smith, Earl Gubbins, Jean Severin and Tom Holzman for the preparation of isotopically labeled FKBP, and Rob Meadows and David Nettesheim for the solvent accessibility data. This research was supported in part by the National Institute of General Medical Sciences (GM45351, awarded to S.W.F.).

REFERENCES

[1] Clore, G.M. and Gronenborn, A.M. (1991) Science 252, 1390–1399.
[2] Montelione, G.T., Winkler, M.E., Rauenbuehler, P. and Wagner, G. (1989) J. Magn. Reson. 82, 198–204.
[3] Montelione, G.T. and Wagner, G. (1989) J. Am. Chem. Soc. 111, 5474–5475.
[4] Edison, A.S., Westler, W.M. and Markley, J.L. (1991) J. Magn. Reson. 92, 434–438.
[5] Gemmecker, G. and Fesik, S.W. (1991) J. Magn. Reson. 95, 208–213.
[6] Emerson, S.D. and Montelione, G.T. (1992) J. Am. Chem. Soc. 114, 354–356.
[7] Griesinger, C. and Eggenberger, U. (1992) J. Magn. Reson. 97, 426–434.
[8] Harding, M.W., Galat, A., Uehling, D.E. and Schreiber, S.L. (1989) Nature 341, 758–760.
[9] Siekierka, J.J., Hung, S.H.Y., Poe, M., Lin, C.S. and Sigal, N.H. (1989) Nature 341, 755–757.
[10] Arai, T., Koyama, Y., Suenaga, T. and Honda, H. (1962) J. Antibiotics 15, 231–232.
[11] Hatanaka, H., Kino, T., Miyata, S., Inamura, N., Kuroka, A., Goto, T., Tanaka, H. and Okuhara, M. (1988) J. Antibiotics 41, 1592–1601.
[12] VanDuyne, G.D., Standaert, R.F., Karplus, P.A., Schreiber, S.L. and Clardy, J. (1991) Science 252, 839–842.
[13] Edalji, R., Pilot-Matias, T.J., Pratt, S.D., Egan, D.A., Severin, J.M., Gubbins, E.G., Smith, H., Park, C.H., Petros, A.M., Fesik, S.W., Luly, J., Burres, N.S. and Holzman, T.F. (1992) J. Prot. Chem., in press.
[14] Olejniczak, E.T. and Eaton, H.L. (1990) J. Magn. Reson. 87, 628–632.
[15] Bax, A., Clore, G.M. and Gronenborn, A.M. (1990) J. Magn. Reson. 88, 425–431.
[16] Rucker, S.P. and Shaka, A.J. (1989) Mol. Phys. 68, 509–517.
[17] Griesinger, C., Otting, G., Wüthrich, K. and Ernst, R.R. (1988) J. Am. Chem. Soc. 110, 7870–7872.
[18] Messerle, B.A., Wider, G., Otting, G., Weber, C. and Wüthrich, K. (1989) J. Magn. Reson. 85, 608–613.
[19] Hyberts, S.G., Märki, W. and Wagner, G. (1987) Eur. J. Biochem. 164, 625–635.
[20] Günteri, P., Braun, W., Billeter, M. and Wüthrich, K. (1989) J. Am. Chem. Soc. 111, 3997–4004.
[21] Nilges, M., Clore, G.M. and Gronenborn, A.M. (1990) Biopolymers 29, 813–822.
[22] Janin, J., Wodak, S., Levitt, M. and Maigret, B. (1978) J. Mol. Biol. 125, 357–386.
[23] DeMarco, A., Llinas, M. and Wüthrich, K. (1978) Biopolymers 17, 2727–2742.
[24] Ponder, J.W. and Richards, F.M. (1987) J. Mol. Biol. 193, 775–791.
[25] Bystrov, V.F. (1976) Prog. NMR Spectroscopy 10, 41–81.
[26] Marion, D., Ikura, M., Tschudin, R. and Bax, A. (1989) J. Magn. Reson. 85, 393–399.